Tonkie Khimicheskie Tekhnologii = Fine Chemical Technologies.
2025;20(2):156–166 ISSN 2686-7575 (Online)

UDC 544.032
https://doi.org/10.32362/2410-6593-2025-20-2-156-166
EDN DKIJFP

RESEARCH ARTICLE

The influence of lanthanum content in the Fe_2O_3–Li_2O–$La(OH)_3$ system on phase formation and properties of composite material

Yuliya S. Elkina✉, **Vitaly A. Vlasov, Elena N. Lysenko, Anatoly P. Surzhikov**
National Research Tomsk Polytechnic University, Tomsk, 634050 Russia
✉ *Corresponding author, e-mail: ysm7@tpu.ru*

Abstract

Objectives. To study the effect of varying lanthanum content in the Fe_2O_3–Li_2O–$La(OH)_3$ system on phase formation and corresponding structural and electromagnetic properties of a lithium-ferrite composite material obtained using high-temperature ceramic technology.

Methods. Following the addition of lanthanum occurred at the initial stage of mixing the Fe_2O_3/Li_2CO_3/$La(OH)_3$ components in a certain weight ratio, the obtained samples were sent for preliminary synthesis at a temperature of 900°C for 240 min in an air atmosphere and sintering in a dilatometer at a temperature of 1100°C for 120 min. The microstructure and properties of the sintered composite samples were studied using X-ray phase analysis (XRD), thermogravimetry (TG), differential scanning calorimetry (DSC), and scanning electron microscopy.

Results. XRD analysis confirmed the formation of a two-phase structure following solid-phase synthesis, consisting of the magnetic phase of lithium ferrite $Li_{0.5}Fe_{2.5}O_4$ and the perovskite-like phase $LaFeO_3$. XRD carried out after sintering showed that the high-temperature heating process did not affect the changes in the phase composition of the sample phases. Dilatometric shrinkage curves obtained after sintering showed that the addition of La reduces the rate of compaction of the samples at the stage of their heating. The sintered samples were characterized by a density of 4.34, 3.84, 3.93 g/cm^3 and a porosity of 0.7, 16, and 18%, respectively, having an increased mass content of $La(OH)_3$ at the synthesis stage. A decrease in the grain sizes was also observed. An increase in the amount of lanthanum hydroxide $La(OH)_3$ additive from 0 to 4.4 and 13.9 wt % led to an increase in the concentration of the synthesized $LaFeO_3$ phase in the samples to 4.2 and 16.6 wt %, resulting in decreased specific saturation magnetization values from 59.4 to 58.2 and 49.7 G·cm^3/g and the initial magnetic permeability from 41.6 to 22.8 and 19.5, respectively. TG and DSC showed that high-temperature sintering of lithium ferrite without additives leads to the predominant formation of the disordered β-phase $Li_{0.5}Fe_{2.5}O_4$, which has a reduced Curie temperature of 626°C. This process is associated with a violation of the stoichiometric composition of the samples for lithium and oxygen due to the release of these elements from the samples during high-temperature sintering.

Conclusions. The high values of the Curie temperature of 631°C confirm that the addition of lanthanum during the production of lithium ferrite prevents the violation of the stoichiometric composition of the ferrite during sintering due to the construction of an additional $LaFeO_3$ lattice. The addition of lanthanum was also found to lead to a significant increase in specific electrical resistance from $5 \cdot 10^2$ to $6 \cdot 10^9$ and $1 \cdot 10^{12}$ Ohm·cm, which may be associated with both a change in the microstructure of the samples and a change in their phase composition.

Keywords
lithium ferrite, lanthanum, magnetic properties, electrical properties, structure, rare earth element

Submitted: 11.09.2024
Revised: 08.11.2024
Accepted: 19.02.2025

For citation

Elkina Yu.S., Vlasov V.A., Lysenko E.N., Surzhikov A.P. The influence of lanthanum content in the Fe_2O_3–Li_2O–$La(OH)_3$ system on phase formation and properties of composite material. *Tonk. Khim. Tekhnol. = Fine Chem. Technol*. 2025;20(2):156–166. https://doi.org/10.32362/2410-6593-2025-20-2-156-166

НАУЧНАЯ СТАТЬЯ

Влияние содержания лантана в системе Fe_2O_3–Li_2O–$La(OH)_3$ на фазообразование и свойства композиционного материала

Ю.С. Елькина✉, В.А. Власов, Е.Н. Лысенко, А.П. Суржиков

Национальный исследовательский Томский политехнический университет, Томск, 634050 Россия

✉ *Автор для переписки, e-mail: ysm7@tpu.ru*

Аннотация

Цели. Исследование влияния содержания лантана в системе Fe_2O_3–Li_2O–$La(OH)_3$ на фазообразование, а также структурные и электромагнитные свойства композиционного материала на основе литиевого феррита, полученного с помощью высокотемпературной керамической технологии.

Методы. Введение лантана происходило на начальном этапе смешивания компонентов Fe_2O_3/Li_2CO_3/$La(OH)_3$ в определенном весовом соотношении, затем полученные образцы были направлены на предварительный синтез при температуре 900°C в течение 240 мин в атмосфере воздуха и дальнейшее спекание в дилатометре при температуре 1100°C в течение 120 мин. Методами рентгенофазового анализа (РФА), термогравиметрии (ТГ), дифференциально-сканирующей калориметрии (ДСК), а также сканирующей электронной микроскопии проведено исследование микроструктуры и свойств исследуемых композиционных образцов.

Результаты. Методом РФА установлено, что после твердофазного синтеза происходит образование двухфазной структуры, состоящей из магнитной фазы литиевого феррита $Li_{0.5}Fe_{2.5}O_4$ и перовскитоподобной фазы $LaFeO_3$. Проведение РФА после спекания показало, что процесс высокотемпературного нагрева не оказал влияния на изменения фазового состава образцов. Дилатометрические кривые усадки, полученные во время спекания, показали, что введение La уменьшает скорость уплотнения образцов на стадии их нагрева. Спеченные образцы характеризовались плотностью 4.34, 3.84, 3.93 г/см^3 и пористостью 0.7, 16 и 18% с увеличением на этапе синтеза массового содержания $La(OH)_3$. Также наблюдалось уменьшение размеров зерна. Увеличение количества добавки $La(OH)_3$ с 0 до 4.4 и 13.9 мас. % привело к увеличению в образцах концентрации фазы $LaFeO_3$ до 4.2 и 16.6 мас. %, что явилось причиной снижения значений удельной намагниченности насыщения соответственно с 59.4 до 58.2 и 49.7 Гс·см^3/г и начальной магнитной проницаемости с 41.6 до 22.8 и 19.5. С помощью ТГ и ДСК показано, что высокотемпературное спекание литиевого феррита без добавок приводит к преимущественному формированию разупорядоченной β-фазы $Li_{0.5}Fe_{2.5}O_4$, имеющей заниженное значение температуры Кюри 626°C. Данный процесс связан с нарушением стехиометрического состава образцов по литию и кислороду вследствие выхода данных элементов из образцов во время высокотемпературного спекания.

Выводы. Введение лантана при получении литиевого феррита препятствует во время спекания нарушению стехиометрического состава феррита за счет построения дополнительной решетки $LaFeO_3$, что подтверждено высокими значениями температуры Кюри 631°C. Также установлено, что введение лантана приводит к значительному увеличению удельного электрического сопротивления с $5 \cdot 10^2$ до $6 \cdot 10^9$ и $1 \cdot 10^{12}$ Ом·см, что может быть связано как с изменением микроструктуры образцов, так и с изменением их фазового состава.

Ключевые слова

литиевый феррит, лантан, магнитные свойства, электрические свойства, структура, редкоземельный элемент

Поступила: 11.09.2024
Доработана: 08.11.2024
Принята в печать: 19.02.2025

Для цитирования

Елькина Ю.С., Власов В.А., Лысенко Е.Н., Суржиков А.П. Влияние содержания лантана в системе Fe_2O_3–Li_2O–$La(OH)_3$ на фазообразование и свойства композиционного материала. *Тонкие химические технологии*. 2025;20(2):156–166. https://doi.org/10.32362/2410-6593-2025-20-2-156-166

INTRODUCTION

The number of studies focused on ferrites, including lithium-containing ferrites having various technological applications, continues to grow steadily each year. Due to its high Curie temperature and saturation magnetization, lithium ferrite $Li_{0.5}Fe_{2.5}O_4$ is used in microwave devices, as well as cathode materials in lithium-ion batteries and gas sensors [1–4]. All these applications, in one way or another, rely on a certain combination of magnetic and electrical properties of this ferrite. To achieve such various combinations, metal ions such as Ti, Zn, Ni, Mg, Mn, Co, etc. are added into the lithium ferrite. Studies [5–8] have shown that certain characteristics can be improved by varying different substitution combinations; however, in many cases this leads to a deterioration of other desired characteristics. Therefore, it becomes necessity to develop methods for improving the electrophysical and magnetic properties of lithium ferrites.

Recently, researchers have been actively investigating the properties of various ferrites with rare earth elements [9–13]. Unpaired 4f electrons located in the outer orbital level of rare earth elements play a major role in the occurrence of magnetic anisotropy due to their orbital shape [10]. This means that the addition of such ions as samarium, lanthanum, gadolinium, etc. to spinel ferrites can change their electrical and magnetic properties. At the same time, there are very few studies devoted to the research of the influence of various rare-earth elements on the properties of lithium ferrites.

It is known that in addition to varying the composition of ferrites due to the inclusion of certain components, the method of obtaining ferrites also affects their properties [3, 10, 12, 14–16]. In the case of traditional and widespread ceramic technology, oxides and carbonates are used as starting reagents to produce ferrites. Based on data from [17], it was shown that during solid-phase interaction of Sm_2O_3/Fe_2O_3/Li_2CO_3 reagents in different weight ratios no substituted lithium ferrite phase is formed, but two phases including unsubstituted lithium ferrite $Li_{0.5}Fe_{2.5}O_4$ and $SmFeO_3$ are formed and affect the final properties of the ferrite.

In this study, the structure and properties of lithium ferrite modified with lanthanum were investigated by X-ray diffraction phase analysis (XRD), thermogravimetry (TG), differential scanning calorimetry (DSC) and scanning electron microscopy (SEM) methods.

MATERIALS AND METHODS

The initial reagents for preparation of lanthanum-modified lithium ferrite were iron oxide Fe_2O_3 (pure for analysis, *Vekton*, Russia), lithium carbonate Li_2CO_3 (extra pure 20-2, *Vekton*, Russia) and lanthanum hydroxide $La(OH)_3$ (99.99%, *MOS International Co.*, China). The weight ratios of these components Fe_2O_3/Li_2CO_3/$La(OH)_3$ were 91.5/8.5/0 wt % (sample N0), 87.3/8.3/4.4 wt % (sample N1), and 78.2/7.9/13.9 wt % (sample N2).

Prior to mixing, the powders were dried in an oven for 120 min at 200°C to remove excess moisture. Mixing of these components was carried out in an E-max ball mill (*Retsch*, Germany) using steel balls with a diameter of 5 mm at 300 rpm for 15 min. Next, the samples were compacted by cold pressing in the form of tablets on a PGr-10 manual hydraulic press (*LabTuls*, Russia). Preliminary synthesis of the obtained samples was carried out in a laboratory furnace at 900°C for 240 min in air atmosphere. Then the samples were ground in an agate mortar and 12 wt % polyvinyl alcohol (95.3%, *MCD Chemicals*, China) was added to the obtained powders. Finally, the powders were compacted into tablets and sintered in a DIL 402C dilatometer (*Netzsch*, Germany) at 1100°C for 2 h.

The phase composition of the obtained samples was studied by XRD on an ARL X'TRA diffractometer (*Thermo Fisher Scientific*, Switzerland) using Cu-K_α radiation. The measurement range was 2θ = 10°–90°. Powder Cell 2.5 software with the International Center for Diffraction Data (ICDD[1]) PDF-4+ database was used for phase identification and quantification.

With the help of TG and DSC analyses, the Curie temperature (T_C) and thermal effects during heating of the samples in a thermal analyzer in STA 449C Jupiter (*Netzsch*, Germany) were investigated. The Curie temperature T_C was obtained by differentiating the TG curve of lithium ferrite into a derivative thermogravimetric curve (DTG), whose peak corresponds to the Curie temperature value according to the methodology presented in [18]. The thermal analysis was performed with the application of an external magnetic field during the entire heating process up to 900°C.

The microstructural features of the lithium samples were studied by SEM on a TM-3000 device (*Hitachi*, Japan).

The saturation magnetization (σ_s) was measured at room temperature using an H-04 pulse magnetometer (*TSU*, Russia). The initial magnetic permeability was

[1] URL: http://www.icdd.com. Accessed February 13, 2023.

measured using the inductive method on a Keysight E4980AL precision LCR meter (*Agilent*, USA). The temperature dependence of the electrical resistivity of the samples was measured using the two-probe method according to the method described in [19].

RESULTS AND DISCUSSION

At the first stage of obtaining the composite material, a solid-phase interaction reaction was carried out between the initial components in a certain weight ratio specified in the experimental procedure.

The qualitative and quantitative phase composition of the samples following synthesis was determined from the XRD results (Table 1 and Fig. 1), which confirmed the formation of two distinct phases: spinel phase $Li_{0.5}Fe_{2.5}O_4$ (PDF No. 01-070-5669[1]) and perovskite-like phase with orthorhombic structure $LaFeO_3$ (PDF No. 01-077-99802[1]). The presence of reflexes at $2\theta \approx 15°$, 23°, and 26°, as well as the lattice parameter ~8.33 Å, which are in agreement with literature data [20], indicate the formation of ordered cubic phase α-$Li_{0.5}Fe_{2.5}O_4$ [21].

The formation of the secondary phase proceeds according to the following mechanism (1):

$$Fe_2O_3 + 2La(OH)_3 = 2LaFeO_3 + 3H_2O. \quad (1)$$

The concentration of the secondary phase depends on the content of the added initial reagent $La(OH)_3$ such that, with an increase of the added lanthanum ions, the content of $LaFeO_3$ increases. Thus, on the basis of XRD analysis it can be seen that the reaction of solid-phase interaction between the initial reagents proceeds without the addition of La into the crystal structure of lithium ferrite, that is, the formation of a two-phase composite. Presumably, the reaction in the synthesis process between the initial

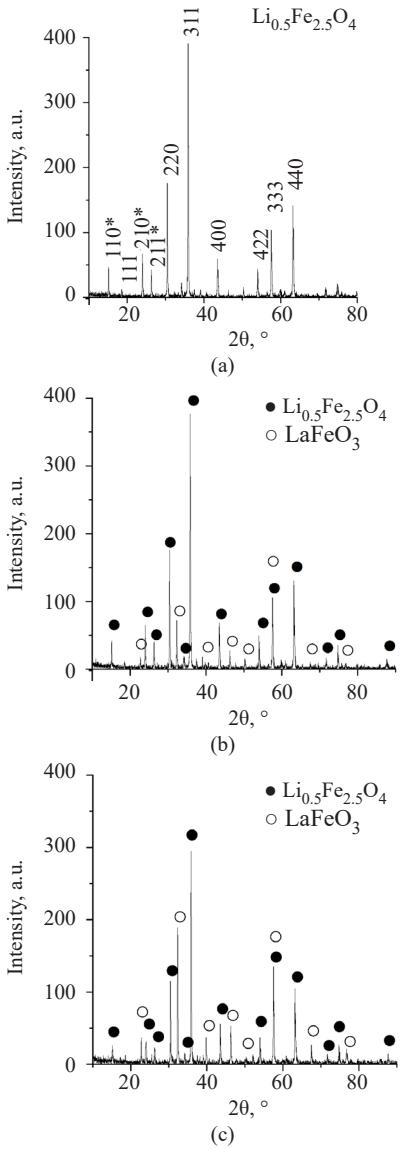

Fig. 1. X-ray diffraction patterns of samples after synthesis, where is (a) N0; (b) N1; (c) N2

Table 1. Phase composition of synthesized samples

Sample	Phase composition	Lattice parameters, Å	Concentration, wt %
N0	$Li_{0.5}Fe_{2.5}O_4$	$a = b = c = 8.3328$ (±0.002)	100
	$LaFeO_3$	–	–
N1	$Li_{0.5}Fe_{2.5}O_4$	$a = b = c = 8.3279$ (±0.002)	95.7
	$LaFeO_3$	$a = 5.5549$ (±0.002) $b = 7.8495$ (±0.003) $c = 5.5477$ (±0.003)	4.3
N2	$Li_{0.5}Fe_{2.5}O_4$	$a = b = c = 8.3310$ (±0.002)	81.9
	$LaFeO_3$	$a = 5.5501$ (±0.002) $b = 7.8613$ (±0.003) $c = 5.5572$ (±0.003)	18.1

reactants $Fe_2O_3/Li_2CO_3/La(OH)_3$ proceeds according to scheme (2):

$$Li_2CO_3 + 6Fe_2O_3 + 2La(OH)_3 = \\ = 4Li_{0.5}Fe_{2.5}O_4 + 2LaFeO_3 + 3H_2O + CO_2. \quad (2)$$

Next, the sintering process was carried out and the dilatometric curves shown in Fig. 2 were obtained.

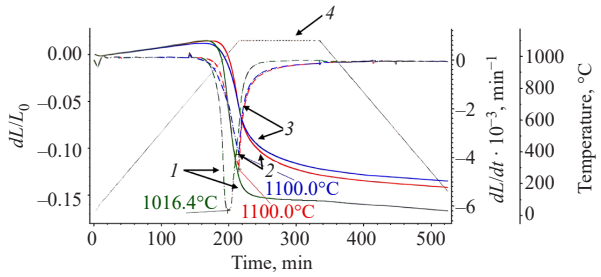

Fig. 2. Dilatometric curves obtained by sintering samples at 1100°C (shrinkage curve—solid lines, shrinkage rate—dotted lines): *1* (green lines) sample N0; *2* (red lines) sample N1; *3* (blue lines) sample N2; *4* temperature program

Up to the temperature of non-isothermal heating 800°C, material expansion occurs in all samples, which is associated with an increase in the volume of gas pores. Then there is a sharp change in the length of samples at a temperature of about 900°C, which is associated with their densification. At the same time, the shrinkage rate of sample N0 is higher than that of N1 and N2. By the end of isothermal curing, sample N0 shows the highest shrinkage. From the shrinkage curves, it can be seen that the addition of lanthanum reduces the shrinkage rate of the samples at the stage of heating and that the shrinkage rate of samples N1 and N2 is almost the same.

The data obtained by measuring the hydrostatic density and porosity indicated in Table 2 confirmed the dilatometry data. With the addition of lanthanum, there is a decrease in density (ρ_{hydr}) and an increase in porosity of samples (Q).

X-ray diffraction patterns of the samples after the sintering process are shown in Fig. 3.

XRD after sintering showed that the qualitative content of phases did not change after this process and that sintered samples contain phases $Li_{0.5}Fe_{2.5}O_4$ and $LaFeO_3$. During sintering (Table 3), the quantitative content of phases in sample N1 practically does not change, while for sample N2 there is a slight decrease in the concentration of $Li_{0.5}Fe_{2.5}O_4$ phase and an increase in the amount of secondary phase $LaFeO_3$ in comparison with the synthesis data.

SEM images of the surface of the samples are shown in Fig. 4. The images of samples N1 and N2, which confirm the conclusions about the formation of a two-phase product after sintering, clearly show two contrasts [17] that correspond to the ferrite phase (gray shade) and

Table 2. Density and porosity of composite samples

Sample	Density ρ_{hydr}, g/cm^3	Porosity Q, %	Grain size D, μm
N0	4.34	0.7	4.78
N1	3.84	16.0	1.63
N2	3.93	18.0	1.57

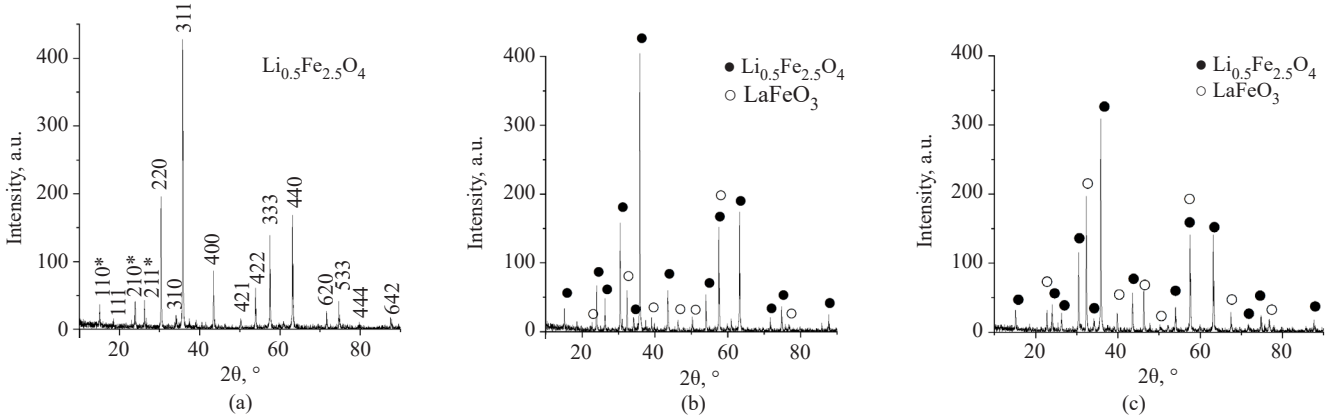

Fig. 3. X-ray diffraction patterns of samples after sintering: (a) N0; (b) N1; (c) N2

Table 3. Phase composition of sintered samples

Sample	Phase composition	Lattice parameters, Å	Concentration, wt %
N0	$Li_{0.5}Fe_{2.5}O_4$	$a = b = c = 8.3327$ (±0.002)	100
	$LaFeO_3$	–	–
N1	$Li_{0.5}Fe_{2.5}O_4$	$a = b = c = 8.3275$ (±0.002)	95.8
	$LaFeO_3$	$a = 5.5506$ (±0.002) $b = 7.8418$ (±0.003) $c = 5.5838$ (±0.003)	4.2
N2	$Li_{0.5}Fe_{2.5}O_4$	$a = b = c = 8.3304$ (±0.002)	83.4
	$LaFeO_3$	$a = 5.5539$ (±0.002) $b = 7.8593$ (±0.003) $c = 5.5535$ (±0.003)	16.6

the $LaFeO_3$ phase (white shade). The addition of La also affects the microstructure of the final ceramic samples. The values of average grain size are given in Table 2. While the addition of La leads to a decrease in the grain size of the ferrite phase [22], the concentration of the rare earth element does not significantly affect the further change of this parameter.

In this work, the electrical resistivity (ρ) was also investigated. The sharp increase in electrical resistivity with increasing additive content shown in Table 4 may be due to an increase in the amount of secondary phase $LaFeO_3$, as well as the high porosity and low density of the samples. Studies of the saturation specific magnetization (σ_s) showed that a slight decrease in this parameter occurs with the addition of La in small amounts. More significant changes occur in the initial magnetic permeability (μ_0) of ferrite [17, 23–27]. This is probably due to the quantitative increase of the $LaFeO_3$ phase, which is antiferromagnetic in nature and behaves as a paramagnetic under certain circumstances.

Furthermore, thermal analysis of the sintered specimens was carried out, the graphs of which are shown in Fig. 5. As shown in [17–19, 21], the thermal endothermic effect on the DSC curve in the temperature

Table 4. Electrical and magnetic properties of samples

Sample	ρ, Ohm·cm	σ_s, G·cm^3/g	μ_0	T_C, °C
N0	$5 \cdot 10^2$	59.4	41.6	626
N1	$6 \cdot 10^9$	58.2	22.8	631
N2	$1 \cdot 10^{12}$	49.7	19.5	630

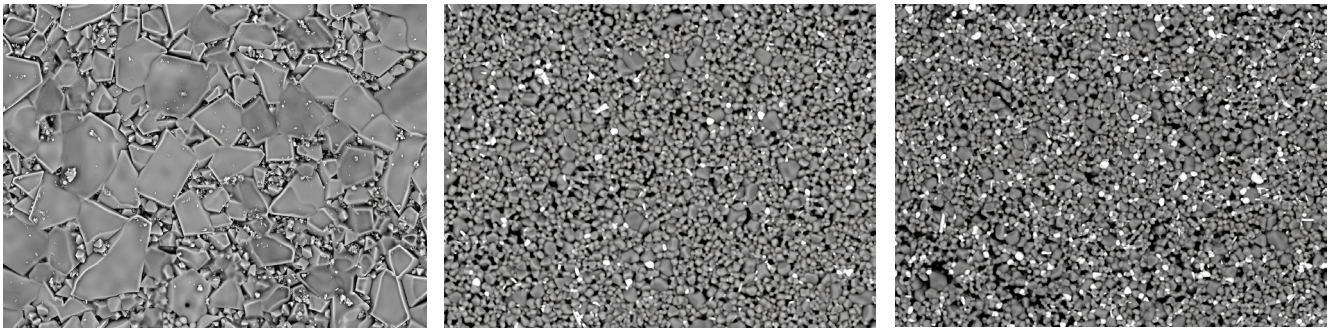

(a) (b) (c)

Fig. 4. SEM images of lithium ferrite modified with lanthanum: (a) N0; (b) N1; (c) N2

region ~700–760°C is associated with the phase transition from the ordered α-phase to the disordered β-phase of the unsubstituted lithium ferrite $Li_{0.5}Fe_{2.5}O_4$.

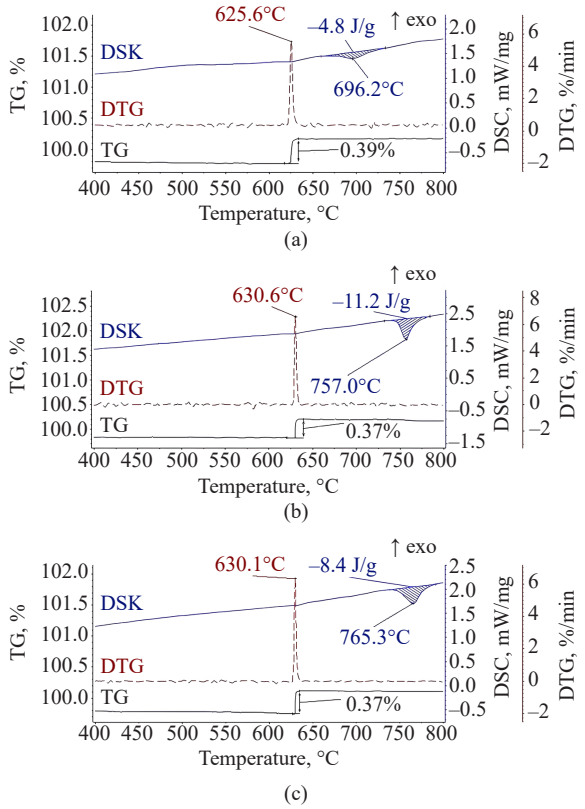

Fig. 5. Thermogravimetric and differential calorimetric curves obtained after sintering at 1100°C

As was shown in [17, 18, 21, 28], the enthalpy of the α→β $Li_{0.5}Fe_{2.5}O_4$ transition is 12–13 J/g according to the peak area of DSC analysis of ferrite. In our study, the value of enthalpy parameter for sample N0 decreased by more than 60%. For samples N1 and N2, the value of enthalpy reduction was about 10 and 30%, respectively. It is also worth noting that with increasing lanthanum content, the temperature range of the thermal effect shifts to higher temperatures from 660–730°C (sample N0) to 732–783°C and 740–790°C for N1 and N2, respectively. Table 3 shows the T_C values for different samples. The T_C value for lithium ferrite N0 is slightly underestimated compared to samples N1 and N2, whose temperature is close to that reported in the studies [17, 18, 21].

It is suggested that the underestimated values of Curie temperature and DSC peak areas in lithium ferrite $Li_{0.5}Fe_{2.5}O_4$ without the addition of lanthanum indicate a disordered ferrite structure during high-temperature sintering due to the loss of oxygen and lithium by the sample [20]. As shown in [18, 21], partial formation of disordered phase β-$Li_{0.5}Fe_{2.5}O_4$ occurs during sintering. The addition of La prevents the disordered stoichiometric composition of sintered lithium ferrite due to the rearrangement of the internal crystal structure.

CONCLUSIONS

In the present study, the influence of lanthanum content in the Fe_2O_3–Li_2O–$La(OH)_3$ system on phase formation is investigated along with the structural and electromagnetic properties of composite material based on lithium ferrite $Li_{0.5}Fe_{2.5}O_4$. The confirmed formation of two-phase composite during the sample synthesis process consists of spinel phase α-$Li_{0.5}Fe_{2.5}O_4$ and perovskite-like phase $LaFeO_3$, whose concentrations depend on the ratios of initial components and do not change significantly during high-temperature sintering.

The study of structural characteristics showed that the increase in lanthanum concentration at the synthesis stage leads to a decrease in density and increase in porosity of sintered samples. The addition of lanthanum also influences the ordering of the ferrite structure during high-temperature sintering to prevent violation of its stoichiometric composition. There is a slight deterioration in magnetic properties and a significant improvement in electrical properties.

The data confirm the utility of small additions of lanthanum as a means of modifying the properties of lithium ferrite with rare-earth elements for potential use in microwave technology.

Further research in this area will be aimed at varying the small amounts of added lanthanum, as well as changing the temperature and time modes of sintering in order to obtain denser and less porous ferrite ceramics offering a good combination of electromagnetic properties.

Acknowledgments

The research was supported by the Ministry of Science and Higher Education of the Russian Federation in part of the science program (project FSWW-2023-0011).

Authors' contributions

Yu.S. Elkina—investigation, methodology, formal analysis, writing the original draft.

V.A. Vlasov—formal analysis, investigation, supervision.

E.N. Lysenko—validation, data curation.

A.P. Surzhikov—conceptualization, funding acquisition.

The authors declare no conflicts of interest.

REFERENCES

1. Ahmad M., Shahid M., Alanazi Y.M., Rehman A. ur., Asif M., Dunnill C.W. Lithium ferrite ($Li_{0.5}Fe_{2.5}O_4$): synthesis, structural, morphological and magnetic evaluation for storage devices. *J. Mater. Res. Technol*. 2022;18:3386–3395. https://doi.org/10.1016/j.jmrt.2022.03.113
2. Khot S.S., Shinde N.S., Basavaiah N., Watawe S.C., Vaidya M.M. Magnetic properties of LiZnCu ferrite synthesized by the microwave sintering method. *J. Magn. Magn. Mater.* 2015;374:182–186. https://doi.org/10.1016/j.jmmm.2014.08.039
3. Aravind G., Raghasudha M., Ravinder D., Manivel Raja M., Meena S.S., Bhatt P., Hashim M. Study of structural and magnetic properties of Li–Ni nanoferrites synthesized by citrate-gel auto combustion. *Ceram. Int.* 2016;42(2): 2941–2950. https://doi.org/10.1016/j.ceramint.2015.10.077
4. Nikishina E.E. Heterophase synthesis of cobalt ferrite. *Fine Chem. Technol*. 2021;16(6):502–511. https://doi.org/10.32362/2410-6593-2021-16-6-502-511
5. Isaev I.M., Kostishin V.G., Korovushkin V.V., *et al.* Magnetic and Radio-Absorbing Properties of Polycrystalline $Li_{0.33}Fe_{2.29}Zn_{0.21}Mn_{0.17}O_4$ Spinel Ferrite. *Tech. Phys.* 2021;66(11):1216–1220. https://doi.org/10.1134/S1063784221090085
[Original Russian Text: Isaev I.M., Kostishin V.G., Korovushkin V.V., Salogub D.V., Shakirzyanov R.I., Timofeev A.V., Mironovich A.Yu. Magnetic and Radio-Absorbing Properties of Polycrystalline $Li_{0.33}Fe_{2.29}Zn_{0.21}Mn_{0.17}O_4$ Spinel Ferrite. *Zhurnal tekhnicheskoi fiziki.* 2021;91(9):1376–1380 (in Russ.). https://doi.org/10.21883/JTF.2021.09.51217.74-21]
6. Isaev I.M., Kostishin V.G., Korovushkin V.V., *et al.* Crystal chemistry and magnetic properties of polycrystalline spinel ferrites $Li_{0.33}Fe_{2.29}Zn_{0.21}Mn_{0.17}O_4$. *Russ. J. Inorg. Chem.* 2021;66(12): 1917–1924. https://doi.org/10.1134/S0036023621120056
[Original Russian Text: Isaev I.M., Kostishin V.G., Korovushkin V.V., Shipko M.N., Timofeev A.V., Mironovich A.Yu., Salogub D.V., Shakirzyanov R.I. Crystal chemistry and magnetic properties of polycrystalline spinel ferrites $Li_{0.33}Fe_{2.29}Zn_{0.21}Mn_{0.17}O_4$. *Zhurnal neorganicheskoi khimii*. 2021;66(12):1792–1800 (in Russ.). https://doi.org/10.31857/S0044457X21120059]
7. Kareva K.V., Suraev A.S., Chervinskaya A.S., Dotsenko O.A., Kushnarev B.O., Minin R.V., Zhuravlev V.A., Wagner D.V. Structural characteristics and magnetic properties of $Ni_{1-x}Zn_xFe_2O_4$ ferrimagnets synthesized by the ceramic method. *Izvestiya vuzov. Fizika*. 2023;66(12):5–11 (in Russ.).
8. Punda A.Yu., Gafarova K.P., Zhivulin V.E., Chernukha A.S., Zykova A.R., Gudkova S.A., Pesin L.A., Vyatkin G.P., Vinnik D.A. Synthesis and structure of barium hexaferrite $BaFe_{12-x}In_xO_{19}$ (x = 0–1). *Zhural obshchei khimii.* 2024;94(2):285–291 (in Russ.). https://doi.org/10.31.57/s0044460x24020149
9. Maksoud M.I.A.A., El-Ghandour A., Ashour A.H., Atta M.M., Abdelhaleem S., El-Hanbaly A.H., Fahim R.A., Kassem S.M., Shalaby M.S., Awed A.S. La^{3+} doped $LiCo_{0.25}Zn_{0.25}Fe_2O_4$ spinel ferrite nanocrystals: Insights on structural, optical and magnetic properties. *J. Rare Earths.* 2021;39(1):75–82. https://doi.org/10.1016/j.jre.2019.12.017
10. Khan M.A., Sabir M., Mahmood A., Asghar M., Mahmood K., Khan M.A., Ahmad I., Sher M., Warsi M.F. High frequency dielectric response and magnetic studies of $Zn_{1-x}Tb_xFe_2O_4$ nanocrystalline ferrites synthesized via micro-emulsion technique. *Magn. Magn. Mater.* 2014;360:188–192. https://doi.org/10.1016/j.jmmm.2014.02.059

СПИСОК ЛИТЕРАТУРЫ

1. Ahmad M., Shahid M., Alanazi Y.M., Rehman A. ur., Asif M., Dunnill C.W. Lithium ferrite ($Li_{0.5}Fe_{2.5}O_4$): synthesis, structural, morphological and magnetic evaluation for storage devices. *J. Mater. Res. Technol*. 2022;18:3386–3395. https://doi.org/10.1016/j.jmrt.2022.03.113
2. Khot S.S., Shinde N.S., Basavaiah N., Watawe S.C., Vaidya M.M. Magnetic properties of LiZnCu ferrite synthesized by the microwave sintering method. *J. Magn. Magn. Mater.* 2015;374:182–186. https://doi.org/10.1016/j.jmmm.2014.08.039
3. Aravind G., Raghasudha M., Ravinder D., Manivel Raja M., Meena S.S., Bhatt P., Hashim M. Study of structural and magnetic properties of Li–Ni nanoferrites synthesized by citrate-gel auto combustion. *Ceram. Int.* 2016;42(2): 2941–2950. https://doi.org/10.1016/j.ceramint.2015.10.077
4. Никишина Е.Е. Гетерофазный синтез феррита кобальта. *Тонкие химические технологии*. 2021;16(6):502–511. https://doi.org/10.32362/2410-6593-2021-16-6-502-511
5. Исаев И.М., Костишин В.Г., Коровушкин В.В., Салогуб Д.В., Шакирзянов Р.И., Тимофеев А.В., Миронович А.Ю. Магнитные и радиопоглощающие свойства поликристаллического феррита-шпинели $Li_{0.33}Fe_{2.29}Zn_{0.21}Mn_{0.17}O_4$. *Журн. техн. физики* (*ЖТФ*). 2021;91(9):1376–1380. https://doi.org/10.21883/JTF.2021.09.51217.74-21
6. Исаев И.М., Костишин В.Г., Коровушкин В.В., Шипко М.Н., Тимофеев А.В., Миронович А.Ю., Салогуб Д.В., Шакирзянов Р.И. Кристаллохимия и магнитные свойства поликристаллических ферритов-шпинелей $Li_{0.33}Fe_{2.29}Zn_{0.21}Mn_{0.17}O_4$. *Журн. неорган. химии.* 2021;66(12):1792–1800. https://doi.org/10.31857/S0044457X21120059
7. Карева К.В., Сураев А.С., Червинская А.С., Доценко О.А., Кушнарев Б.О., Минин Р.В., Журавлев В.А., Вагнер Д.В. Структурные характеристики и магнитные свойства синтезированных керамическим методом ферримагнетиков $Ni_{1-x}Zn_xFe_2O_4$. *Известия вузов. Физика.* 2023;66(12):5–11.
8. Пунда А.Ю., Гафарова К.П., Живулин В.Е., Чернуха А.С., Зыкова А.Р., Гудкова С.А., Песин Л.А., Вяткин Г.П., Винник Д.А. Синтез и структура гексаферрита бария $BaFe_{12-x}In_xO_{19}$ (x = 0–1). *Журн. общей химии*. 2024;94(2): 285–291. https://doi.org/10.31857/s0044460x24020149
9. Maksoud M.I.A.A., El-Ghandour A., Ashour A.H., Atta M.M., Abdelhaleem S., El-Hanbaly A.H., Fahim R.A., Kassem S.M., Shalaby M.S., Awed A.S. La^{3+} doped $LiCo_{0.25}Zn_{0.25}Fe_2O_4$ spinel ferrite nanocrystals: Insights on structural, optical and magnetic properties. *J. Rare Earths.* 2021;39(1):75–82. https://doi.org/10.1016/j.jre.2019.12.017
10. Khan M.A., Sabir M., Mahmood A., Asghar M., Mahmood K., Khan M.A., Ahmad I., Sher M., Warsi M.F. High frequency dielectric response and magnetic studies of $Zn_{1-x}Tb_xFe_2O_4$ nanocrystalline ferrites synthesized via micro-emulsion technique. *Magn. Magn. Mater.* 2014;360:188–192. https://doi.org/10.1016/j.jmmm.2014.02.059
11. Ahmad I., Abbas T., Ziya A.B., Maqsood A. Structural and magnetic properties of erbium doped nanocrystalline Li–Ni ferrites. *Ceram. Int.* 2014;40(6):7941–7945. https://doi.org/10.1016/j.ceramint.2013.12.142
12. Jiang J., Liangchao L., Feng X. Structural analysis and magnetic properties of Gd-doped Li-Ni ferrites prepared using rheological phase reaction method. *J. Rare Earths.* 2007;25(1):79–83. https://doi.org/10.1016/S1002-0721(07)60049-0
13. Mahmoudi M., Kavanlouei M., Maleki-Ghaleh H. Effect of composition on structural and magnetic properties of nanocrystalline ferrite $Li_{0.5}Sm_xFe_{2.5-x}O_4$. *Powd. Metall. Met. Ceram.* 2015;54: 31–39. https://doi.org/10.1007/s11106-015-9676-9

11. Ahmad I., Abbas T., Ziya A.B., Maqsood A. Structural and magnetic properties of erbium doped nanocrystalline Li–Ni ferrites. *Ceram. Int.* 2014;40(6):7941–7945. https://doi.org/10.1016/j.ceramint.2013.12.142
12. Jiang J., Liangchao L., Feng X. Structural analysis and magnetic properties of Gd-doped Li-Ni ferrites prepared using rheological phase reaction method. *J. Rare Earths.* 2007;25(1):79–83. https://doi.org/10.1016/S1002-0721(07)60049-0
13. Mahmoudi M., Kavanlouei M., Maleki-Ghaleh H. Effect of composition on structural and magnetic properties of nanocrystalline ferrite $Li_{0.5}Sm_xFe_{2.5-x}O_4$. *Powd. Metall. Met. Ceram.* 2015;54:31–39. https://doi.org/10.1007/s11106-015-9676-9
14. Nikumbh A.K., Pawar R.A., Nighot D.V., Gugale G.S., Sangale M.D., Khanvilkar M.B., Nagawade A.V. Structural, electrical, magnetic and dielectric properties of rare-earth substituted cobalt ferrites nanoparticles synthesized by the co-precipitation method. *J. Magn. Magn. Mater.*2014;355:201–209. https://doi.org/10.1016/j.jmmm.2013.11.052
15. Sadykov S.A., Kallaev S.N., Emirov R.M., Alikhanov N.M.-R. Electrical properties of Sm- doped $BiFeO_3$ ceramics. *Phys. Solid State.*2023;65(10):1654–1663. https://doi.org/110.61011/PSS.2023.10.57217.149
[Original Russian Text: Sadykov S.A., Kallaev S.N., Emirov R.M., Alikhanov N.M.-R. Electrical properties of Sm-doped $BiFeO_3$ ceramics. *Fizika tverdogo tela.* 2023;65(10):1727–1736 (in Russ.). https://doi.org/10.61011/FTT.2023.10.56320.149]
16. Khabirov R.R., Mass A.V., Kuzmin R.I., Ruktuev A.A., Cherkasova N.Yu., Agafonov M.Yu., Koroleva V.A., Miller A.A. Features of the formation of the structure and properties of Mn–Zn ferrites obtained by sol-gel synthesis. *Tech. Phys. Lett*. 2024;50(9):17–21. https://doi.org/10.61011/TPL.2024.05.58414.19834
[Original Russian Text: Khabirov R.R., Mass A.V., Kuzmin R.I., Ruktuev A.A., Cherkasova N.Yu., Agafonov M. Yu., Koroleva V.A., Miller A.A. Features of the formation of the structure and properties of Mn–Zn ferrites obtained by sol-gel synthesis. *Pis'ma v Zhurnal tekhnicheskoi fiziki*. 2024;50(9):21–26 (in Russ.). https://doi.org/10.61011/PJTF.2024.09.57563.19834]
17. Lysenko E.N., Vlasov V.A., Nikolaeva S.A., Nikolaev E.V. TG, DSC, XRD, and SEM studies of the substituted lithium ferrite formation from milled $Sm_2O_3/Fe_2O_3/Li_2CO_3$ precursors. *J. Therm. Anal. Calorim.* 2023;148(4):1445–1453. https://doi.org/10.1007/s10973-022-11665-1
18. Lysenko E.N., Surzhikov A.P., Astafyev A.L. Thermomagnetometric analysis of lithium ferrites. *J. Therm. Anal. Colorim*. 2019;136(2):441–445. https://doi.org/10.1007/s10973-018-7678-9
19. Lysenko E.N., Nikolaeva S.A., Surzhikov A.P., Ghyngazov S.A., Plotnikova I.V., Zhuravlev A., Zhuravleva E.V. Electrical and magnetic properties of ZrO_2-doped lithium-titanium-zinc ferrite ceramics. *Ceram. Int.* 2019;45(16):20148–20154. https://doi.org/10.1016/j.ceramint.2019.06.282
20. Ridley D.H., Lessoff H., Childress J.D. Effect of lithium and oxygen losses on magnetic and crystallographic properties of spinel lithium ferrite. *J. Am. Ceram. Soc.* 1970;53(6):304–311. https://doi.org/10.1111/J.1151-2916.1970.TB12113.X
21. Surzhikov A.P., Frangulyan T.S., Ghyngazov S.A., Lysenko E.N. Investigation of structural states and oxidation processes in $Li_{0.5}Fe_{2.5}O_{4-\delta}$ using TG analysis. *J. Therm. Anal. Calorim.* 2012;108(3):1207–1212. https://doi.org/10.1007/s10973-011-1734-z
14. Nikumbh A.K., Pawar R.A., Nighot D.V., Gugale G.S., Sangale M.D., Khanvilkar M.B., Nagawade A.V. Structural, electrical, magnetic and dielectric properties of rare-earth substituted cobalt ferrites nanoparticles synthesized by the co-precipitation method. *J. Magn. Magn. Mater.*2014;355:201–209. https://doi.org/10.1016/j.jmmm.2013.11.052
15. Садыков С.А., Каллаев С.Н., Эмиров Р.М., Алиханов Н.М.-Р. Электрические свойства керамики $BiFeO_3$, легированной Sm. *Физика твердого тела.* 2023;65(10):1727–1736. https://doi.org/10.61011/FTT.2023.10.56320.149
16. Хабиров Р.Р., Масс А.В., Кузьмин Р.И., Руктуев А.А., Черкасова Н.Ю., Агафонов М.Ю., Королева В.А., Миллер А.А. Особенности формирования структуры и свойств Mn–Zn-ферритов, полученных методом золь-гель синтеза. *Письма в ЖТФ*. 2024;50(9):21–26. https://doi.org/10.61011/PJTF.2024.09.57563.19834
17. Lysenko E.N., Vlasov V.A., Nikolaeva S.A., Nikolaev E.V. TG, DSC, XRD, and SEM studies of the substituted lithium ferrite formation from milled $Sm_2O_3/Fe_2O_3/Li_2CO_3$ precursors. *J. Therm. Anal. Calorim.* 2023;148(4):1445–1453. https://doi.org/10.1007/s10973-022-11665-1
18. Lysenko E.N., Surzhikov A.P., Astafyev A.L. Thermomagnetometric analysis of lithium ferrites. *J. Therm. Anal. Colorim*. 2019;136(2):441–445. https://doi.org/10.1007/s10973-018-7678-9
19. Lysenko E.N., Nikolaeva S.A., Surzhikov A.P., Ghyngazov S.A., Plotnikova I.V., Zhuravlev A., Zhuravleva E.V. Electrical and magnetic properties of ZrO_2-doped lithium-titanium-zinc ferrite ceramics. *Ceram. Int.* 2019;45(16):20148–20154. https://doi.org/10.1016/j.ceramint.2019.06.282
20. Ridley D.H., Lessoff H., Childress J.D. Effect of lithium and oxygen losses on magnetic and crystallographic properties of spinel lithium ferrite. *J. Am. Ceram. Soc.* 1970;53(6):304–311. https://doi.org/10.1111/J.1151-2916.1970.TB12113.X
21. Surzhikov A.P., Frangulyan T.S., Ghyngazov S.A., Lysenko E.N. Investigation of structural states and oxidation processes in $Li_{0.5}Fe_{2.5}O_{4-\delta}$ using TG analysis. *J. Therm. Anal. Calorim.* 2012;108(3):1207–1212. https://doi.org/10.1007/s10973-011-1734-z
22. Bulai G., Diamandescu L., Dumitru I., Gurlui S., Feder M., Caltun O.F., Effect of rare earth substitution in cobalt ferrite bulk materials. *J. Magn. Magn. Mater*. 2015;390:123–131. https://doi.org/10.1016/j.jmmm.2015.04.089
23. Mohanty V., Cheruku R., Vijayan L., Govindaraj G. Ce-substituted Lithium Ferrite: Preparation and Electrical Relaxation Studies. *J. Mater. Sci. Technol*. 2014;30(4):335–341. https://doi.org/10.1016/j.jmst.2013.10.028
24. Al-Hilli M.F., Li S., Kassim K.S. Structural analysis, magnetic and electrical properties of samarium substituted lithium–nickel mixed ferrites. *J. Magn. Magn. Mater*. 2012;324(5):873–879. https://doi.org/10.1016/j.jmmm.2011.10.005
25. An S.Y., Shim I.B., Kim C.S. Synthesis and magnetic properties of $LiFe_5O_8$ powders by a sol–gel process. *J. Magn. Magn Mater.* 2005;290–291:1551–1554. https://doi.org/10.1016/j.jmmm.2004.11.244
26. Mazen S.A., Abu-Elsaad N.I. Characterization and magnetic investigations of germanium-doped lithium ferrite. *Ceram. Int.* 2014;40(7):11229–11237. https://doi.org/10.1016/j.ceramint.2014.03.167
27. Abdellatif M.H., El-Komy G.M., Azab A.A., Magnetic characterization of rare earth doped spinel ferrite. *J. Magn. Magn. Mater*. 2017;442:445–452. https://doi.org/10.1016/j.jmmm.2017.07.020

22. Bulai G., Diamandescu L., Dumitru I., Gurlui S., Feder M., Caltun O.F., Effect of rare earth substitution in cobalt ferrite bulk materials. *J. Magn. Magn. Mater*. 2015;390:123–131. https://doi.org/10.1016/j.jmmm.2015.04.089
23. Mohanty V., Cheruku R., Vijayan L., Govindaraj G. Ce-substituted Lithium Ferrite: Preparation and Electrical Relaxation Studies. *J. Mater. Sci. Technol*. 2014;30(4): 335–341. https://doi.org/10.1016/j.jmst.2013.10.028
24. Al-Hilli M.F., Li S., Kassim K.S. Structural analysis, magnetic and electrical properties of samarium substituted lithium–nickel mixed ferrites. *J. Magn. Magn. Mater*. 2012;324(5):873–879. https://doi.org/10.1016/j.jmmm.2011.10.005
25. An S.Y., Shim I.B., Kim C.S. Synthesis and magnetic properties of $LiFe_5O_8$ powders by a sol–gel process. *J. Magn. Magn Mater.* 2005;290–291:1551–1554. https://doi.org/10.1016/j.jmmm.2004.11.244
26. Mazen S.A., Abu-Elsaad N.I. Characterization and magnetic investigations of germanium-doped lithium ferrite. *Ceram. Int.* 2014;40(7):11229–11237. https://doi.org/10.1016/j.ceramint.2014.03.167
27. Abdellatif M.H., El-Komy G.M., Azab A.A., Magnetic characterization of rare earth doped spinel ferrite. *J. Magn. Magn. Mater*. 2017;442:445–452. https://doi.org/10.1016/j.jmmm.2017.07.020
28. Berbenni V., Marini A., Capsoni D. Solid state reaction study of the system Li_2CO_3/Fe_2O_3. *Z. Naturforschung – Sect. J. Phys. Sci.* 1998;53:997–1003. https://doi.org/10.1515/zna-1998-1212

28. Berbenni V., Marini A., Capsoni D. Solid state reaction study of the system Li_2CO_3/Fe_2O_3. *Z. Naturforschung – Sect. J. Phys. Sci.* 1998;53:997–1003. https://doi.org/10.1515/zna-1998-1212

About the Authors

Yuliya S. Elkina, Postgraduate Student, Research Laboratory for Electronics, Semiconductors and Dielectrics, Research School of High-Energy Physics, Tomsk Polytechnic University (30, Lenina pr., Tomsk, 634034, Russia). E-mail: ysm7@tpu.ru. Scopus Author ID 58892380200, ResearcherID HHS-0003-2022, RSCI SPIN-code 6717-1540, https://orcid.org/0000-0002-2708-9872

Vitaly A. Vlasov, Cand. Sci. (Phys.-Math.), Senior Researcher, Research Laboratory for Electronics, Semiconductors and Dielectrics, Research School of High-Energy Physics, Tomsk Polytechnic University (30, Lenina pr., Tomsk, 634034, Russia). E-mail: vlvitan@tpu.ru. Scopus Author ID 7202194125, ResearcherID K-1257-2013, RSCI SPIN-code 2003-8431, https://orcid.org/0000-0002-5946-2117

Elena N. Lysenko, Dr. Sci. (Eng.), Professor, Head of the Laboratory, Research Laboratory for Electronics, Semiconductors and Dielectrics, Research School of High-Energy Physics, Tomsk Polytechnic University (30, Lenina pr., Tomsk, 634034, Russia). E-mail: lysenkoen@tpu.ru. Scopus Author ID 25027787100, ResearcherID K-1582-2013, RSCI SPIN-code 6536-9390, https://orcid.org/0000-0002-5093-2207

Anatoly P. Surzhikov, Dr. Sci. (Phys.-Math.), Professor, Head of the Department, Division for Testing and Diagnostics, School of Non-Destructive Testing, Tomsk Polytechnic University (30, Lenina pr., Tomsk, 634034, Russia). surzhikov@tpu.ru. Scopus Author ID 6603494148, ResearcherID K-1224-2013, RSCI SPIN-code 1875-0293, https://orcid.org/0000-0003-2795-398X

Об авторах

Елькина Юлия Сергеевна, аспирант, проблемная научно-исследовательская лаборатория электроники диэлектриков и полупроводников, Исследовательская школа физики высокоэнергетических процессов, ФГАОУ ВО «Национальный исследовательский Томский политехнический университет» (634050, Россия, г. Томск, пр. Ленина, д. 30). E-mail: ysm7@tpu.ru. Scopus Author ID 58892380200, ResearcherID HHS-0003-2022, SPIN-код РИНЦ 6717-1540, https://orcid.org/0000-0002-2708-9872

Власов Виталий Анатольевич, к.ф.-м.н., старший научный сотрудник, проблемная научно-исследовательская лаборатория электроники диэлектриков и полупроводников, Исследовательская школа физики высокоэнергетических процессов, ФГАОУ ВО «Национальный исследовательский Томский политехнический университет» (634050, Россия, г. Томск, пр. Ленина, д. 30). E-mail: vlvitan@tpu.ru. Scopus Author ID 7202194125, ResearcherID K-1257-2013, SPIN-код РИНЦ 2003-8431, https://orcid.org/0000-0002-5946-2117

Лысенко Елена Николаевна, д.т.н., профессор, заведующая лабораторией, проблемная научно-исследовательская лаборатория электроники диэлектриков и полупроводников, Исследовательская школа физики высокоэнергетических процессов, ФГАОУ ВО «Национальный исследовательский Томский политехнический университет» (634050, Россия, г. Томск, пр. Ленина, д. 30). E-mail: lysenkoen@tpu.ru. Scopus Author ID 25027787100, ResearcherID K-1582-2013, SPIN-код РИНЦ 6536-9390, https://orcid.org/0000-0002-5093-2207

Суржиков Анатолий Петрович, д.ф.-м.н., профессор, заведующий кафедрой – руководитель отделения на правах кафедры, отделение контроля и диагностики, Инженерная школа неразрушающего контроля и безопасности, ФГАОУ ВО «Национальный исследовательский Томский политехнический университет» (634050, Россия, г. Томск, пр. Ленина, д. 30). E-mail: surzhikov@tpu.ru. Scopus Author ID 6603494148, ResearcherID K-1224-2013, SPIN-код РИНЦ 1875-0293, https://orcid.org/0000-0003-2795-398X

Translated from Russian into English by H. Moshkov
Edited for English language and spelling by Thomas A. Beavitt